ISSN 1674-1056
http://cpb.iphy.ac.cn
http://iopscience.iop.org/cpb
中国物理 B
Chinese Physics
中国物理
Chinese Physics B

Numerical simulation on modulational instability of ion-acoustic wave in plasma

Yi-Rong Ma(马艺荣), Lie-Juan Li(李烈娟), Wen-Shan Duan(段文山)

Citation: Chin. Phys. B . 2019, 28(2): 025201. **doi:** 10.1088/1674-1056/28/2/025201
Journal homepage: http://cpb.iphy.ac.cn; http://iopscience.iop.org/cpb

What follows is a list of articles you may be interested in

Acceleration and radiation of externally injected electrons in laser plasma wakefield driven by a Laguerre-Gaussian pulse

Zhong-Chen Shen(沈众辰), Min Chen(陈民), Guo-Bo Zhang(张国博), Ji Luo(罗辑), Su-Ming Weng(翁苏明), Xiao-Hui Yuan(远晓辉), Feng Liu(刘峰), Zheng-Ming Sheng(盛政明)

Chin. Phys. B . 2017, 26(11): 115204. **doi:** 10.1088/1674-1056/26/11/115204

Modeling of nonlinear envelope solitons in strongly coupled dusty plasmas: Instability and collision

S. K. El-Labany, E. F. El-Shamy, W. F. El-Taibany, N. A. Zedan

Chin. Phys. B . 2015, 24(3): 035201. **doi:** 10.1088/1674-1056/24/3/035201

Relativistic degenerate effects of electrons and positrons on modulational instability of quantum ion acoustic waves in dense plasmas with two polarity ions

Liu Tie-Lu, Wang Yun-Liang, Lu Yan-Zhen

Chin. Phys. B . 2015, 24(2): 025202. **doi:** 10.1088/1674-1056/24/2/025202

Effect of inner-surface roughness of conical target on laser absorption and fast electron generation

Wang Huan, Cao Li-Hua, Zhao Zong-Qing, Yu Ming-Yang, Gu Yu-Qiu, He Xian-Tu

Chin. Phys. B . 2014, 23(5): 055202. **doi:** 10.1088/1674-1056/23/5/055202

Using short pulses to enhance the production rate of vibrationally excited hydrogen molecules in hydrogen discharge

Sun Ji-Zhong,Li Xian-Tao,Bai Jing,Wang De-Zhen

Chin. Phys. B . 2012, 21(5): 055205. **doi:** 10.1088/1674-1056/21/5/055205

Numerical simulation on modulational instability of ion-acoustic waves in plasma*

Yi-Rong Ma(马艺荣)[1,2], Lie-Juan Li(李烈娟)[2], and Wen-Shan Duan(段文山)[2,†]

[1] Center for Quantum Technology Research, School of Physics, Beijing Institute of Technology, Beijing 100081, China
[2] College of Physics and Electronic Engineering, Joint Laboratory of Atomic and Molecular Physics of NWNU & IMP CAS, Northwest Normal University, Lanzhou 730070, China

(Received 16 October 2018; revised manuscript received 29 November 2018; published online 10 January 2019)

In this paper, the one-dimensional (1D) particle-in-cell (PIC) simulation is used to study the modulation instability of ion acoustic waves in electron–ion plasmas. The ion acoustic wave is described by using a nonlinear Schrödinger equation (NLSE) derived from the reductive perturbation method. Form our numerical simulations, we are able to demonstrate that, after the modulation, the amplitude increases steadily over time. Furthermore, by comparing the numerical results with traditional analytical solutions, we acquire the application scope for the reductive perturbation method to obtain the NLSE. We also find this method can also be extended to other fields such as fluid dynamics, nonlinear optics, solid state physics, and the Bose–Einstein condensate to validate the application scope of the results from the traditional perturbation method.

Keywords: modulational instability, particle-in-cell simulation, the reductive perturbation method

PACS: 52.27.Aj, 52.35.–g, 52.65.Rr **DOI:** 10.1088/1674-1056/28/2/025201

1. Introduction

As one of the most important subjects in the study of plasma physics, nonlinear wave propagation in plasmas has received a lot of attention. In recent research work, the problems of nonlinear waves propagating in plasmas is described by using the nonlinear Schrodinger equation (NLSE). Unlike the Korteweg–de Vries (KdV) equation, which describes the evolution of long wavelength and small amplitude waves, the NLSE governs the dynamics of a modulated wave packet.[1–3] For a medium with a positive coefficient of the nonlinearity term in the NLSE, an instability that takes place in the longitudinal direction is referred to as the modulational instability. Even when a modulation of the wave mode takes place in a direction diagonal to the direction of the carrier wave propagation, this instability could still be called a modulational instability.[4–6]

In particular, there exists a modulation instability mechanism that can describe the evolution of a wave through the nonlinear Schrödinger equation[7]

$$\mathrm{i}\frac{\partial \Phi}{\partial \tau} + P\frac{\partial \Phi}{\partial \xi^2} + Q|\Phi|^2\Phi = 0, \tag{1}$$

where the modulational instability depends on the coefficient product PQ, this may be investigated in terms of the characteristic parameters involved in a physical system. For $PQ > 0$, the amplitude is said to be unstable against external perturbations. If $PQ < 0$, it is modulationally stable. This modulation instability mechanism is synonymous to the Benjamin–Feir instability which is an energy localization mechanism typically used in the area of solid state physic, nonlinear optics, and hydrodynamics. Due to this, the modulational stability can be investigated in terms of characteristic parameters, including the wave number k. Presently, investigations into some electrostatic (ES) modes have already been investigated.[8,9]

To date, the modulational instability of different wave modes in plasmas has received a great deal of interest,[10–13] for example, the modulational instability of the monochromatic ion–acoustic wave (IAW) has generally been described using the NLSE from the resultant equations of the reductive perturbation theory.[14–16] Their corresponding experimental observations were first reported by Watanabe.[17,18] For two-component plasmas that comprise singly charged positive ions and electrons, much of the theoretical efforts have focused on investigating the modulational instability of ion–acoustic wave (IAW). In earlier works, Hasegawa considered the modulational instability of an IAW when the modulation took place diagonal to the propagation direction of a carrier wave.[19] Soon after, Chhabra and Sharm investigated the modulational instability of ion–acoustic waves in a plasma comprising two-ion species with singly ionized positive ions.[20] Mishra *et al.* studied the modulational instability of obliquely modulated ion–acoustic waves in a collisionless plasma containing two-ion species with different masses, concentrations, and charged states.[21,22] Additionally, the modulational instability has been researched by various simulation methods[23,24] in a variety of different plasma media, including dusty plasmas.[25–29]

When initial disturbances in the plasma take place for cer-

*Project supported by the National Natural Science Foundation of China (Grant No. 11675014).
†Corresponding author. E-mail: duanws@126.com
© 2019 Chinese Physical Society and IOP Publishing Ltd

tain periods of time, a solitary wave can be created. The amplitude of an excited solitary wave, however, depends on the type and strength of the initial disturbances. In the present paper, we attempt to investigate ion acoustic waves obtained though the reductive perturbation method and discuss modulational instability in the plasma using the one-dimensional electrostatic particle-in-cell (PIC) method.[30,31] This method is a common numerical simulation method used to solve certain classes of partial differential equations. At the beginning of the simulation, super-particles (SPs) are uniformly distributed throughout the region of interest,where each SPs is given a weight factor S that specifies the number of real particles represented. When the properties of SPs are taken into account and weighed on the x grid, the electronic field $\boldsymbol{E}$ has the ability to move the SPs according to Newton's equations of motion:

$$m_{\rm sp}\frac{{\rm d}\boldsymbol{v}_{\rm sp}}{{\rm d}t}=q_{\rm sp}\boldsymbol{E},\quad \frac{{\rm d}\boldsymbol{x}_{\rm sp}}{{\rm d}t}=\boldsymbol{v}_{\rm sp}, \tag{2}$$

where $m_{\rm sp}$, $\boldsymbol{v}_{\rm sp}$, $q_{\rm sp}$, and $\boldsymbol{x}_{\rm sp}$ refer to the mass, velocity, charge, and position of the SPs, respectively. The procedure repeats the solution in Eq. (2) by a leap-frog algorithm and the numerical results are obtained under certain boundary conditions.

A comparison of the numerical results with the analytical results is then the final step in the process. Typically, ion acoustic waves have the maximum dimensionless amplitude and propagation speed when influenced by certain perturbation periods. Furthermore, the reductive perturbation method is only valid when small parameters ϵ and wave numbers k correspond to specific values.

This paper is organized as follows: In Section 1, the reductive perturbation method is used to derive the NLSE governing the dynamics of obliquely modulated IAW, introduced in Section 2. Section 3 presents a brief introduction of the modulation and the PIC method. A comparison between the numerical and analytical results is discussed in Section 4. Finally, we offer our conclusions in Section 5.

2. A derivation of the nonlinear Schrödinger equation using the reductive perturbation method

We consider a one-dimensional, collisionless plasma composed of electrons and ions. For this situation, the nonlinear dynamics of the system is described by

$$\frac{\partial n_{\rm i}}{\partial t}+\frac{\partial}{\partial x}(n_{\rm i}v_{\rm i})=0, \tag{3}$$

$$\frac{\partial v_{\rm i}}{\partial t}+v_{\rm i}\frac{\partial v_{\rm i}}{\partial x}=-Z\frac{\partial\phi}{\partial x}, \tag{4}$$

$$\frac{\partial^2\phi}{\partial x^2}=\mu\,{\rm e}^{\phi}-Zn_{\rm i} \tag{5}$$

where $n_{\rm i}$, $v_{\rm i}$, and ϕ represent the number density of ions, the velocity of the ion fluid, and the self-consistent electrostatic potential, respectively. Z is the charge number of an ion. μ equals $n_{\rm e0}/n_{\rm i0}$, while $n_{\rm e0}$ and $n_{\rm i0}$ are the unperturbed ions and electron number densities, respectively.

All physical quantities are normalized as follows: n_i is normalized using $n_{\rm i0}$. The space coordinates x are normalized by the ion Debye length $\lambda_{\rm Di}=[T_{\rm e}/4\pi n_{\rm i0}\,{\rm e}^2]^{1/2}$, where $T_{\rm e}$ is the thermal energy of the electrons. Moreover, $v_{\rm i}$ is normalized by the ion–acoustic speed $c_{\rm si}[=(T_{\rm e}/m_{\rm i})^{1/2}]$, the mass of ions $m_{\rm i}$ by the proton mass m_p, ϕ by $T_{\rm e}/e$ and t by the ion plasma period $\omega_{\rm pi}^{-1}[(=4\pi n_{\rm i0}\,{\rm e}^2)^{-1/2}]$.

To obtain the NLSE, new stretched coordinates are introduced:

$$\xi=\epsilon(x-v_st),\quad \tau=\epsilon^2t, \tag{6}$$

where ϵ is a small dimensionless parameter, and $v_{\rm s}$ is the group velocity of ion acoustic waves. The variables $n_{\rm i}$, $v_{\rm i}$, and ϕ can then be expanded as

$$\begin{aligned} n_{\rm i} &= 1+\sum_{m=1}^{\infty}\epsilon^m\sum_{l=-\infty}^{\infty}n_l^{(m)}\,{\rm e}^{{\rm i}lX},\\ v_{\rm i} &= \sum_{m=1}^{\infty}\epsilon^m\sum_{l=-\infty}^{\infty}v_l^{(m)}\,{\rm e}^{{\rm i}lX},\\ \phi &= \sum_{m=1}^{\infty}\epsilon^m\sum_{l=-\infty}^{\infty}\phi_l^{(m)}\,{\rm e}^{{\rm i}lX}, \end{aligned} \tag{7}$$

where k is the wave number and ω is the wave frequency. In the new coordinate system, we let

$$X=kx-\omega t=\frac{k}{\epsilon}\xi+\left(\frac{kv_{\rm s}-\omega}{\epsilon^2}\right)\tau. \tag{8}$$

By substituting these expansions into Eqs. (3)–(5), we obtain various powers of ϵ giving the following equations in the lowest order

$$n_1^{(1)}=\frac{k}{\omega}v_1^{(1)},\quad n_{-1}^{(1)}=\frac{k}{\omega}v_{-1}^{(1)}, \tag{9}$$

$$v_1^{(1)}=Z\frac{k}{\omega}\phi_1^{(1)},\quad v_{-1}^{(1)}=\frac{k}{\omega}\phi_{-1}^{(1)} \tag{10}$$

and

$$\omega^2=\frac{Z^2k^2}{\mu+k^2},\quad V_{\rm s}=\frac{k}{\omega}-\frac{\omega^3}{Z^2k}. \tag{11}$$

For ϵ in the higher order, we then obtain the nonlinear Schrödinger equation

$${\rm i}\frac{\partial\phi_1^{(1)}}{\partial\tau}+P\frac{\partial\phi_1^{(1)}}{\partial\xi^2}+Q|\phi_1^{(1)}|^2\phi_1^{(1)}=0, \tag{12}$$

where the dispersion coefficient P and nonlinear coefficient Q found in Eq. (12) are given by

$$\begin{aligned} P &= \frac{3\omega^3(\omega^2-1)}{2k^2}\sim P(k),\\ Q &= -\frac{\omega^3}{2Zk^2}\left[\frac{2Zk^2}{\omega^3}(B_{02}+B_{22})+\frac{Zk^2}{\omega^2}(A_{02}+A_{22})\right. \end{aligned} \tag{13}$$

$$-\frac{\mu}{Z}(C_{02}+C_{22})\Big] \sim Q(k) \tag{14}$$

with

$$A_{02} = Z\frac{\mu v_s^2\omega^3 - Z^3k^2(\omega+2v_sk)}{v_s^2\omega^3(Z^2-\mu v_s^2)} + Z^2\frac{k^2(\omega+2v_sk)}{v_s^2\omega^3}, \tag{15}$$

$$B_{02} = Z\frac{\mu v_s^2\omega^3 - Z^3k^2(\omega+2v_sk)}{v_s^2\omega^3(Z^2-\mu v_s^2)} + Z^2\frac{k^2}{v_s\omega^2}, \tag{16}$$

$$C_{02} = \frac{\mu v_s^2\omega^3 - Z^3k^2(\omega+2v_sk)}{\omega^3(Z^2-\mu v_s^2)}, \tag{17}$$

$$A_{22} = Z\frac{k^2(\mu\omega^4+3Z^4k^4)}{2\omega^4[Z^2k^2-(\mu+4k^2)\omega]} + Z^3\frac{3k^4}{2\omega^4}, \tag{18}$$

$$B_{22} = Z\frac{k(\mu\omega^4-3Z^3k^4)}{2\omega^3[Z^2k^2-(\mu+4k^2)\omega]} + Z^2\frac{k^3}{2\omega^3}, \tag{19}$$

$$C_{22} = \frac{k(\mu\omega^4-3Z^3k^4)}{2\omega^3[Z^2k^2-(\mu+4k^2)\omega]}. \tag{20}$$

For the NLSE of Eq. (12), a well-known solution is given as follows:

$$\phi_1^{(1)} = \phi_0\, e^{iQ|\phi_0|^2\tau}, \tag{21}$$

where ϕ_0 is the amplitude of the lowest order in the expansion of ϕ. By substituting Eq. (21) into Eq. (7) and taking the lowest-order approximation into account, we obtain n_i, v_i, and ϕ by

$$\begin{aligned}
\phi &= \epsilon\phi_0 \exp\left\{i\left[\frac{k}{\epsilon}\xi + (Q|\phi_0|^2 + \frac{kv_s-\omega}{\epsilon^2})\tau\right]\right\},\\
v_i &= \epsilon\frac{k}{\omega}\phi_0 \exp\left\{i\left[\frac{k}{\epsilon}\xi + (Q|\phi_0|^2 + \frac{kv_s-\omega}{\epsilon^2})\tau\right]\right\},\\
n_i &= 1+\epsilon\frac{k^2}{\omega^2}\phi_0 \exp\left\{i\left[\frac{k}{\epsilon}\xi + (Q|\phi_0|^2 + \frac{kv_s-\omega}{\epsilon^2})\tau\right]\right\}.
\end{aligned} \tag{22}$$

3. Stability analysis and the particle-in-cell (PIC) method

Firstly, we study the stability of the wave solution of the NLSE obtained above by adding modulation to the wave in the propagation direction. To do this, we separate the amplitude ϕ_0 into two parts

$$\phi_0 = \phi_{00} + \epsilon'\phi_{10}\, e^{i(\hat{k}\xi-\hat{\omega}\tau)}, \tag{23}$$

where $\hat{k} \ll k$ and $\hat{\omega} \ll \omega$ are the wave number and the frequency of the modulation, respectively. $\epsilon' \ll 1$ is another small parameter. So $\hat{\xi} = \hat{k}\xi - \hat{\omega}\tau$ is the modulation phase, ϕ_{00} is the quantity without modulation and $\epsilon'\phi_{10}$ is the small amplitude of the modulation. Then equation (21) can then be rewritten as

$$\phi_1^{(1)} = \phi_{00}\, e^{iQ|\phi_0|^2\tau} + \epsilon'\phi_{10}\, e^{i[\hat{k}\xi+(Q|\phi_0|^2-\hat{\omega})\tau]}. \tag{24}$$

In this instance, equation (22) is accordingly adapted to the following form in the laboratory coordinates

$$\begin{aligned}
\phi &= \epsilon\phi_{00}\, e^{i[kx+(Q|\phi_0|^2\epsilon^2-\omega)t]}\\
&\quad + \epsilon\epsilon'\phi_{10}\, e^{i[(\hat{k}\epsilon+k)x+(Q|\phi_0|^2\epsilon^2-\omega-\hat{\omega}\epsilon^2-\hat{k}\epsilon v_s)t]},\\
v_i &= \epsilon\frac{k}{\omega}\phi_{00}\, e^{i[kx+(Q|\phi_0|^2\epsilon^2-\omega)t]}\\
&\quad + \epsilon\epsilon'\frac{k}{\omega}\phi_{10}\, e^{i[(\hat{k}\epsilon+k)x+(Q|\phi_0|^2\epsilon^2-\omega-\hat{\omega}\epsilon^2-\hat{k}\epsilon v_s)t]},\\
n_i &= 1+\epsilon\frac{k^2}{\omega^2}\phi_{00}\, e^{i[kx+(Q|\phi_0|^2\epsilon^2-\omega)t]}\\
&\quad + \epsilon\epsilon'\frac{k^2}{\omega^2}\phi_{10}\, e^{i[(\hat{k}\epsilon+k)x+(Q|\phi_0|^2\epsilon^2-\omega-\hat{\omega}\epsilon^2-\hat{k}\epsilon v_s)t]}.
\end{aligned} \tag{25}$$

Substituting Eq. (23) into Eq. (12) and separating the real and imaginary parts, we obtain the nonlinear dispersion relation:

$$\hat{\omega}^2 = P^2\hat{k}^2\cdot\left(\hat{k}^2 - 2\frac{Q}{P}|\phi_0|^2\right). \tag{26}$$

When $PQ > 0$ ($k > 1.403$, see in Fig. 1), then $\hat{\omega}$ will have an imaginary quantity (*i.e.*, $\hat{\omega} = a + ib$, where $a(\hat{k})$ and $b(\hat{k})$ are real-valued functions). For a small value of $\hat{k}$ the amplitude will increase according to $\phi_{00} + \epsilon'\phi_{10}\, e^{|b|t}$. In other words, the wave is modulationally unstable to long wavelength perturbations for the modulation wave number $\hat{k}$.

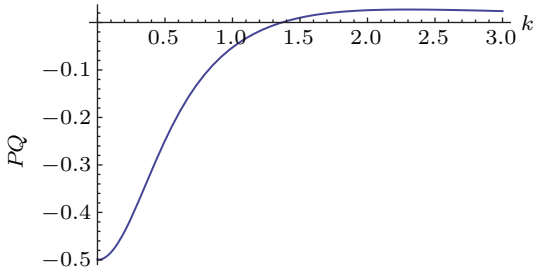


Fig. 1. Dependence of The product of the dispersion coefficient P and the nonlinear coefficients Q on the wave number k.

Next we use the 1D PIC simulation method to accomplish the numerical calculation results. We then set the simulation parameters as follows: $\Delta x = \pi/10$, $\Delta t = \Delta x/100$, the number of grid cells is equal to $N = 1.8\times10^4$, and the quantity of super particles contained within a cell is 100. The parameters ϵ, v_s, k, $\hat{k}$, ω, and $\hat{\omega}$ were evaluated in the following situations. Moreover, we took the periodic boundary conditions along the x axis to avoid any wave reflections.

4. Results and discussion

This section displays all PIC simulations. Figure 2 shows the time evolution of the ion acoustic waves in the form given by Eq. (23). In this figure, the corresponding solution is shown to evolve steadily over time, where the higher order modulation (belonging to the original ion acoustic wave) can be seen. It is noted analytically from Eq. (24) that modulational instability exists if the wave number k satisfies $k > 1.403$, that is, the amplitude increases slightly in a short amount of time as a result of modulation, as shown in Fig. 2. To validate this, figure 3 presents the variation in wave amplitude over time for

two cases having different parameters k. In this case, the parameters $\epsilon = 0.02$, $\phi_{00} = 0.1$, $\phi_{10} = 0.01$, and $\hat{k} = 0.1$ were used. As shown in Fig. 3, when $k = 1.4$, the wave is stable as the amplitude shows near independence on the time t. However, when $k = 1.5$, the wave amplitude is shown to increase over time t.

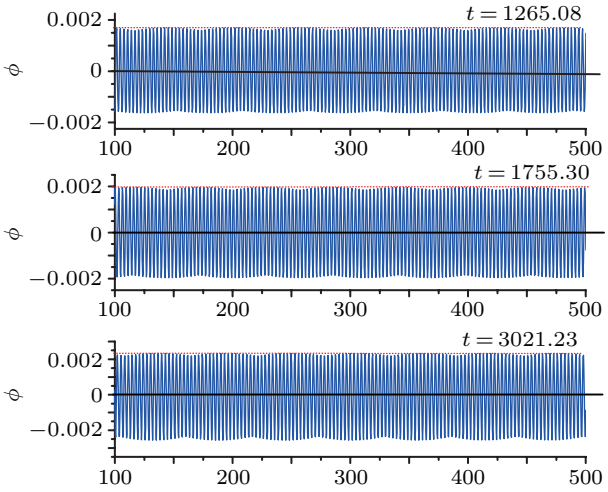


Fig. 2. The PIC simulation results for the evolution of wave amplitude at different time points using $\epsilon = 0.02$ and $k = 1.5$.

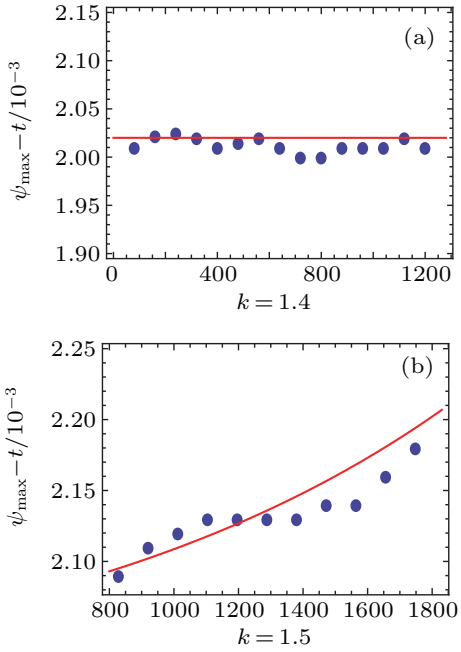


Fig. 3. The variation in amplitude $\phi_{\max}$ with respect to time. $k = 1.4$ is in panel (a) and $k = 1.5$ is in panel (b). The parameters used are $\epsilon = 0.02$, $\phi_{00} = 0.1$, $\phi_{10} = 0.01$, and $\hat{k} = 0.1$. The red line indicates the analytical results obtained. The dotted line indicates the numerical results.

In order to gain further insight into the effects of parameter k on the wave character, variations to both wave amplitude and propagation speed with respect to k are shown in Fig. 4, where the values of the parameters are similar to those in Fig. 3. Note from Fig. 4 that the amplitude increases as k increases, while it attends to a limitation value if k further increases. On the other hand, the wave speed decreases as k increases.

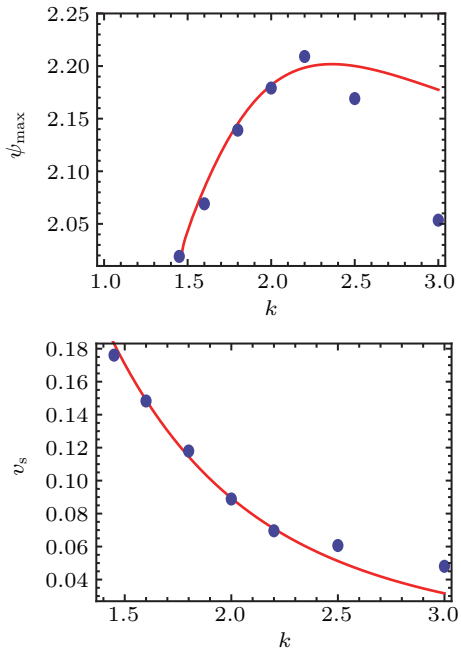


Fig. 4. The dependence of wave amplitude and propagation speed on the wave number k, where $\epsilon = 0.02$, $\phi_{00} = 0.1$, $\phi_{10} = 0.01$, and $\hat{k} = 0.1$. The blue points represent the PIC numerical results and the red line represent the analytical results.

We also want to know if $\hat{k}$ affects the wave character. Figure 5 shows the dependence of the maximum amplitude $\phi_{\max}$ on different wave number $\hat{k}$ of the modulational wave, where $k = 2.0$ and $\epsilon = 0.02$. It is noted from Fig. 5 that for the same ion acoustic wave, its incremental quantity increases as the wave number $\hat{k}$ increases. Moreover, figure 6 shows that the maximum amplitude of the solitary waves will also increase as the parameter ϵ increases.

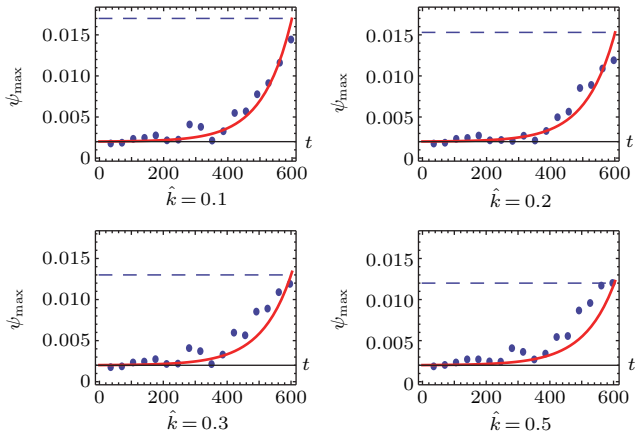


Fig. 5. The dependence of the envelope solitary wave amplitude $\phi_{\max}$ on time t. Here $k = 2.0$, $\phi_{00} = 0.1$, $\phi_{10} = 0.05$, and $k = 2.0$. The blue points represent the PIC numerical results and the red line represent the analytical results.

The comparisons between PIC numerical results and the analytical ones are also given in Figs. 3–6. Especially in Fig. 4 we note that when $k < 2.5$, the differences between analytical results and the numerical ones are small. However, the differences between two become larger if $k > 3$. Figure 6 shows that the differences between analytical results and the numerical ones is negligibly small when $\epsilon < 0.01$ and then it will

increase as ϵ increases. These results infer that the application scope of the analytical solution using the reductive perturbation method mainly depends on both the plasma parameter k and the value of the small parameter ϵ. In order to get more insight into how the small parameter ϵ and ϵ' affect the relative difference between numerical results and the analytical ones, the relative differences are shown in Fig. 7. It can be noted that the relative difference between numerical results and the analytical solution increase substantially as ϵ and ϵ' increase. It will be found that the perturbation method should be applied in the region where both parameters of ϵ and ϵ' are much smaller than unity, especially if the small parameters satisfied $\epsilon < 0.02$ and $\epsilon' < 0.15$, the relative difference can be kept within 0.1.

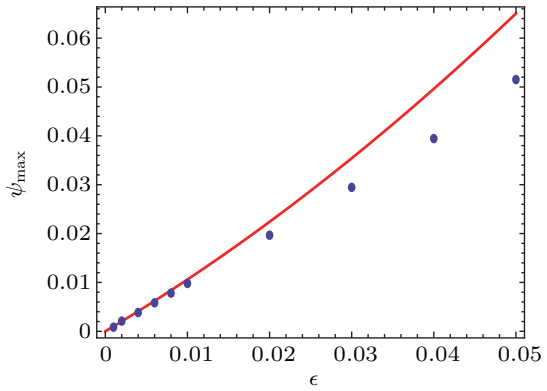


Fig. 6. The dependence of the envelope solitary wave amplitude $\phi_{\max}$ on the ϵ parameter, where $k = 2.0$, $\phi_{00} = 0.1$, $\phi_{10} = 0.01$, and $\hat{k} = 0.1$. The blue points represent the PIC numerical results and the red line represent the analytical results.

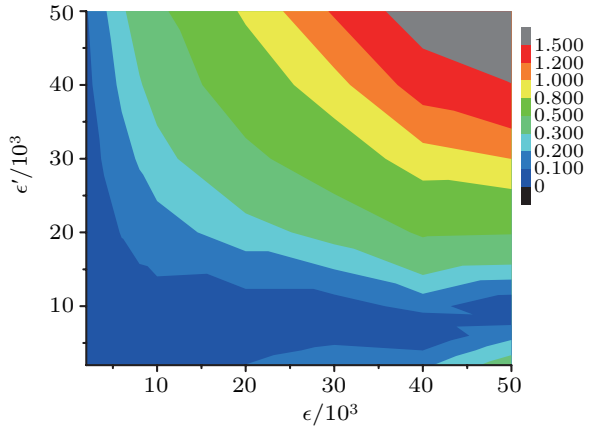


Fig. 7. The relative difference between numerical and analytical results in regards to the small parameter ϵ and ϵ', when $k = 1.8$, $\phi_{00} = 0.1$, $\phi_{10} = 0.01$, and $\hat{k} = 0.05$.

5. Conclusion

By using the 1D PIC method we study the modulational instability of the ion acoustic waves in plasmas composed of cold ions and hot electrons. It is found that the evolution of a wave depends on the dispersion coefficient P and dispersion coefficient Q, both of which are functions of the wave number k. If $k > 1.403PQ > 0$, then the carrier wave is unstable to external perturbations, which is verified by our numerical simulation in the present paper.

After comparing the PIC numerical results with the analytical ones of the reductive perturbation method, the application scope of the reductive perturbation method is clarified. It is found that the application range of the perturbation method in this plasma depends on the value of the small parameters used in the perturbation study.

Since the reductive perturbation method has been widely used in solving nonlinear differential equations in lots of physical problems such as fluid dynamics, plasma physics, nonlinear optics, and Bose–Einstein condensates (BEC) system, the application scope of the reductive perturbation method by using the numerical simulation can also be used in these system.

References

[1] Misra A P and Chowdhury A R 2006 *Eur. Phys. J. D* **37** 105
[2] Xue J and Lang H 2003 *Phys. Plasmas* **10** 339
[3] Zhao C, Gao Y T, Lan Z Z, Yang J W and Su C Q 2016 *Mod. Phys. Lett. B* **13** 1650312
[4] Amin M R, Morfill G E and Shukla P K 1998 *Phys. Rev. E* **58** 6517
[5] Chhabra R S and Sharma S R 1986 *Phys. Fluids* **29** 128
[6] Verheest F 2000 *Waves and instabilities in dusty space plasmas* (Dordrech: Kluwer Academic Publishers) pp. 127–147
[7] Delande D and Sacha K 2014 *Phys. Rev. Lett.* **112** 040402
[8] Zhang H, Qi X, Duan W S and Yang L 2015 *Sci. Rep.* **5** 14239
[9] Remoissenet M 1996 *Waves Called Solitons* (New York: Springer-Verlag) pp. 88–122
[10] Rao N N, Shukla P K and Yu M Y 1990 *Planet. Space Sci.* **38** 543
[11] Shukla P K and Silin V P 1992 *Phys. Scr.* **45** 508
[12] Kourakis I, Esfandyari-Kalejahi A, Mehdipoor M and Shukla P K 2006 *Phys. Plasmas* **13** 052117
[13] Mahmood S, Siddiqui S and Jehan N 2011 *Phys. Plasmas* **18** 052309
[14] Fried B D and Gould R W 1961 *Phys. Fluids* **4** 139
[15] Qi X, Xu Y X, Zhao X Y, Zhang L Y, Duan W S and Yang L 2015 *IEEE Trans. Plasma Sci.* **43** 3815
[16] Taniuti T and Yajima N 1969 *J. Math. Phys.* **10** 1369
[17] Watanabe S 1977 *J. Plasma Phys.* **17** 487
[18] Couede L, Nosenk V, Ivlev A V, Zhdanov S K, Thomas H M and Morfill G E 2010 *Phys. Rev. Lett.* **104** 195001
[19] Hasegawa A 1989 *Modulational Instability* (Berlin, Heidelberg: Springer) pp. 56–62
[20] Yashvir, Bhatnagar T N and Sharma S R 1985 *J. Plasma Phys.* **33** 209
[21] Mishra M K, Chhabra R S and Sharma S R 1994 *Phys. Plasmas* **1** 70
[22] Stenflo L, Shukla P K and Tsintsadze N L 1994 *Phys. Lett. A* **191** 159
[23] Birdsall C K and Langdon A B 1985 *Plasma Physics via Computer Simulation* (New York: McGraw-Hill) Part. 2
[24] Qi X, Xu Y X, Duan W S and Yang L 2014 *Phys. Plasmas* **21** 013702
[25] Misra A P and Chowdhury A R 2006 *Phys. Plasmas* **13** 072305
[26] Bains A, Tribeche M and Ng C S 2013 *Astrophys. Space Sci.* **343** 621
[27] Kourakis I and Shukla P K 2003 *Phys. Plasmas* **10** 3459
[28] Kourakis I and Shukla P K 2005 *Nonlinear Processes in Geophysics* **12** 407
[29] El-Taibany W F, El-Bedwehy N A and El-Shamy E F 2011 *Plasma Phys.* **18** 033703
[30] Liu W Y, Luo W, Yuan T, Yu J Y and Chen M 2018 *Chin. Phys. B* **27** 105202
[31] Liu C S, Han H Y, Peng X Q 2010 *Chin. Phys. B* **19** 035201